Arbitrary-dimensional teleportation of optical number states with linear optics

T. Farrow[1, 2, *] and V. Vedral[1, 2]

[1] *Atomic and Laser Physics, Clarendon Laboratory, University of Oxford, Parks Road, Oxford, OX1 3PU, United Kingdom*

[2] *Centre for Quantum Technologies, National University of Singapore, 3 Science Drive 2, 117543, Singapore*

(Dated: May 4, 2016)

Quantum state teleportation of optical number states is conspicuously absent from the list of experimental milestones achieved to date [1]. Here we demonstrate analytically a teleportation scheme with fidelity 100% for optical number states of arbitrary dimension using linear optical elements only. To this end, we develop an EPR source to supply Bell-type states for the teleportation, and show how the same set-up can also be used as a Bell-state analyser (BSA) when implemented in a time-reversal manner. These two aspects are then brought together to complete the teleportation protocol in a scheme that can deliver perfect fidelity, albeit with an efficiency that decays exponentially as the occupation of the number states increases stepwise. The EPR source and BSA schemes both consist of two optical axes in a symmetrical V-shape experimental layout, along which beam-splitters are placed cross-beam fashion at regular intervals, with their transmittivities treated as variables for which the values are calculated *ad hoc*. In particular, we show the full treatment for the case of qutrit teleportation, and calculate the transmittivity values of the beam splitters required for teleporting qubits, qutrits, qupentits, quheptits and qunits. The general case for arbitrary-dimensional number state teleportation is demonstrated through a counting argument.

arXiv:1605.00970v1 [quant-ph] 3 May 2016

Photons (interchangeably referred to as optical number-states or Fock-states) are bosons. Unlike fermionic electrons, they have the property that they can fly undisturbed since they do not interact with each other. This can be used to great advantage particularly in areas such as quantum communication and information processing where an ideal transmission medium would have the property that it could carry information without degrading it, i.e. that the received information would have a perfect fidelity of 1. In this respect, photons represent the medium of choice and offer significant advantages over electronic channels. But since they do not interact, they are also difficult to control (compared to electrons).

This paper offers a generalisation of the teleportation protocol to an arbitrary dimension of optical number states. Its generality sets it apart from previous teleportation schemes. The first laboratory implementations of teleportation, performed by Bouwmeester et al. [2] and Boschi et al. [3], succeeded in teleporting a photon's polarisation state, that is, an internal degree of freedom. A more general scheme was implemented by Furusawa et al. [21], where a coherent state of light was teleported via continuous variables [4], that is, a subset of the spatial degree of freedom. A third and more general type of teleportation was realised for a single optical number state in superposition with the vacuum state [5]. We take this as our starting point, and extend the idea of number state teleportation to arbitrarily large states.

Introducing teleportation

Since teleportation was first introduced as a concept in 1993 [6] it has also been implemented in trapped ions ([7] -[11]), cold atomic ensembles ([12] -[15]), solid state and NMR systems ([16] - [20]), as well as in optical-modes ([21] -[29]), photonic polarisation ([2], [30]-[35]) and spin-orbital angular momenta states ([36]). It offers a fundamentally new method of transferring quantum information between two particles separated by an arbitrary distance, currently over 140km in free space [37]. For the scheme to work, the two particles must be in a non-local superposition of quantum states, otherwise known as entanglement, a notion that came with the Einstein-Rosen-Podolsky (EPR) paradox [38]. Within the context of a teleportation scheme, two entangled particles are said to form a *quantum channel*, as opposed to a classical one. A corollary is the fact that all operations performed in a teleportation protocol are *local*, so that no measurements need be carried out on all the states in the system simultaneously.

A fundamental distinction between teleportation and classical communication stems from the *no-cloning theorem* [39] in quantum mechanics, which states that no *copy* of a quantum state can be made. Note that this does not mean a quantum state cannot be *transferred* from one particle to another, but merely that a reproduction of it cannot

*Electronic address: tristan.farrow@physics.ox.ac.uk

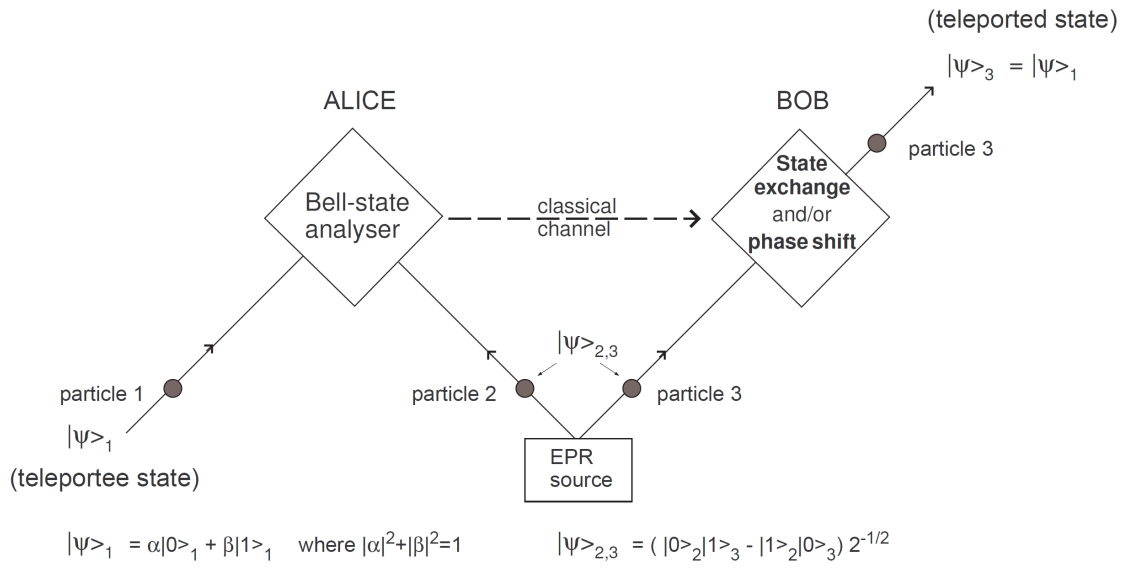

FIG. 1: Protocol for teleporting a pure quantum state from particle 1, i.e. a linear superposition of qubits between logical 0 and 1 describing the state of the particle, to particle 3 some distance away. Particle 3 is generated by an EPR source jointly with particle 2 in a maximally entangled singlet state described by $|\Psi\rangle_{2,3}$, which establishes a quantum communication channel. The result of the Bell-state Analysis [40] performed by Alice is communicated to Bob via a classical channel, who then recovers the state on particle 3, thus completing the teleportation. The initial state on particle 1 is destroyed (maximally mixed).

coexist with the original. In practise this means that during a teleportation, the initial quantum state is destroyed, by becoming maximally mixed, so that at the end we are not left with any copies of the state with which we started. Rather, only the teleported state remains, and this will have been transferred across to the recipient particle where it will now reside, as illustrated in figure 1. Unlike classical communication, teleportation is not a facsimile process.

Generating maximally entangled states with linear optics: EPR source

To generate maximally entangled states with linear optics [41], we propose a set-up consisting of beam splitters placed along two branches in a symmetrical "V" layout, as shown in figure 2. Each branch contains an equal number of beam-splitters while their transmittivities *along* each branch are treated as variables (from T_θ for the first beam-splitter, up to $T_{\phi_{n-1}}$ for the last). Beam-splitters at the same distance along the two branches have the same transmittivity. An equal number of photons is injected into the inputs of the two branches (labelled 1 and 2), and *only* the outcomes that result in single photons emerging from all outputs *except* the two outermost (labelled $1'$ and $2'$) are selected. Provided each of the detectors along the two branches registers a single photon, then we can be sure that the possible combination of output states in modes $1'$ and $2'$ will range from

$$|2n\rangle_{1'}|0\rangle_{2'}, |2n-1\rangle_{1'}|1\rangle_{2'}, \ldots, |1\rangle_{1'}|2n-1\rangle_{2'}, |0\rangle_{1'}|2n\rangle_{2'} \tag{1}$$

where $|n\rangle$ is the number state injected into each of the two branches. A laboratory implementation of the scheme would require single-photon detection devices to be located along all the side-outputs of the two branches, as shown in figure 2. Apart from the qubit, we consider only even number inputs of photons, although the scheme can be extended to assymmetric inputs too.

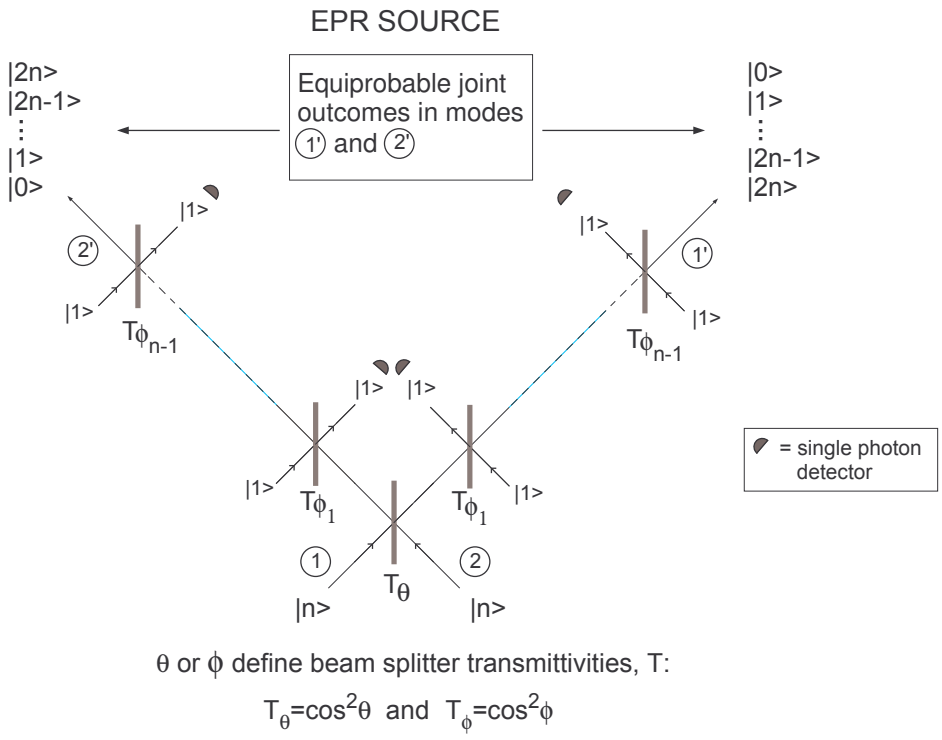

FIG. 2: Generic schematic of our proposed EPR source. A symmetric photon input is injected into channels 1 and 2, and we sub-select *only* the outcomes (i.e. the set of states and their amplitudes) that result in single photons emerging from all outputs *except* the two outermost (labelled $1'$ and $2'$). An implementation of the scheme would have to rely on single-photon detection schemes.

Each outcome, or state, in equation (1) will have associated with it a probability amplitude as a function of the transmittivities of the beam-splitter in the two branches:

$$|State\rangle_{out} = A|2n\rangle_{1'}|0\rangle_{2'} + B|2n-1\rangle_{1'}|1\rangle_{2'} + \ldots + C|n\rangle_{1'}|n\rangle_{2'} + D|1\rangle_{1'}|2n-1\rangle_{2'} + E|0\rangle_{1'}|2n\rangle_{2'} \tag{2}$$

where A, B, C, D, E represent expressions for the amplitudes in terms of variables T_θ to $T_{\phi_{n-1}}$. We note that since they represent the probability amplitudes of a sub-selection of possible outcomes, we normalise them so that $|A|^2 + |B|^2 + |C|^2 + |D|^2 + |E|^2 = 1$. For example, let us imagine that we have five expressions for A to E, then a set of two independent simultaneous equations can be formed ($A = B$ and $B = C$), which can then be solved for the transmittivity values. At these values, the probability amplitudes are equal, since $A = B = C$, while by symmetry $D = B$ and $E = A$. The resulting sum of the state vectors is then our maximally entangled state. Note that we only need a simultaneous solution to the first three expressions (A, B, C) due to the symmetry of our system, which ensures automatically that $B = D$ and $A = E$, meaning that symmetrical outcomes, say, $|2n\rangle_{1'}|0\rangle_{2'}$ and $|0\rangle_{1'}|2n\rangle_{2'}$, are equally likely.
The total number of beam splitters in each branch (including the first beam-splitter shared by the two branches) equals the number of photons injected into each branch. If a symmetrical input of $|n\rangle_1$ photons is injected into branch 1 and $|n\rangle_2$ into branch 2, then the total number of beam-spitters will be $2n - 1$, including the shared first element.

A general counting argument follows, together with a method for calculating the transmittivities that produce maximally entangled states. Larger input states rapidly become too onerous for analytical treatment, so warrant numerical simulation.

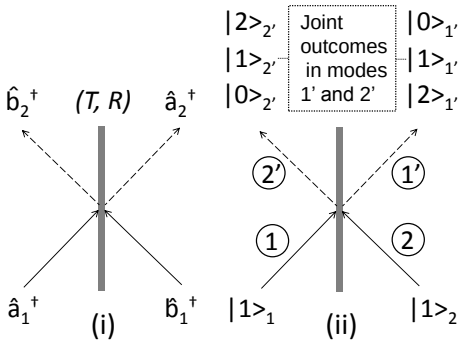

FIG. 3: (i) Beam splitter with transmittivity T and reflectivity R, where $T + R = 1$ since $T = cos^2\theta$ and $R = sin^2\theta$. In the operator model, the unitary transformation due to a beam splitter on an optical mode can be expressed algebraically as $\hat{a_1}^\dagger \overset{bs}{\longmapsto} \cos\theta \hat{a_2}^\dagger + \sin\theta \hat{b_2}^\dagger$ and $\hat{b_1}^\dagger \overset{bs}{\longmapsto} -\sin\theta \hat{a_2}^\dagger + \cos\theta \hat{b_2}^\dagger$, where the input and output modes $\hat{a}^\dagger$ and $\hat{b}^\dagger$ are shown in the figure. This can be represented as a matrix to highlight the beam splitter's mapping function and unitarity. (ii) EPR source: using an asymmetric beam-splitter the outcome $|11\rangle_{1',2'}$ can be achieved with equal probability as $|20\rangle_{1',2'}$ and $|02\rangle_{1',2'}$.

Input $|1\rangle_1|1\rangle_2$

For an input consisting of one photon on each input mode, we have

$$|1\rangle|1\rangle \equiv \hat{a}^\dagger\,\hat{b}^\dagger\,|0\rangle|0\rangle$$

$$\overset{bs}{\longmapsto} \left(\sqrt{T}\,\hat{c}^\dagger + \sqrt{R}\,\hat{d}^\dagger\right)\left(-\sqrt{R}\,\hat{c}^\dagger + \sqrt{T}\,\hat{d}^\dagger\right)|0\rangle|0\rangle$$

$$= \left(T\,\hat{a}^\dagger\hat{b}^\dagger - \sqrt{TR}(\hat{a}^\dagger)^2 + \sqrt{TR}(\hat{b}^\dagger)^2 - R\hat{b}^\dagger\hat{a}^\dagger\right)|0\rangle|0\rangle$$

$$= \left((T-R)\,\hat{a}^\dagger\hat{b}^\dagger + \sqrt{TR}\left(\hat{b^\dagger}^2 - \hat{a^\dagger}^2\right)\right)|0\rangle|0\rangle$$

$$\therefore\ |1\rangle_1|1\rangle_2 \overset{bs}{\longmapsto} (T-R)\,|1\rangle_{1'}|1\rangle_{2'} + \sqrt{TR}\,\sqrt{2}\left(|0\rangle_{1'}|2\rangle_{2'} - |2\rangle_{1'}|0\rangle_{2'}\right) \tag{3}$$

For $T = R$, the output $|1\rangle_{1'}|1\rangle_{2'}$ does not arise, while $|0\rangle_{1'}|2\rangle_{2'}$ and $|2\rangle_{1'}|0\rangle_{2'}$ are equiprobable. In this scenario, the resulting superposition is not a Bell-type state. For maximum entanglement, we require that all the amplitude prefactors in equation (3) be equal. Hence we form the simultaneous equations (4) and (5) which we solve for T and R. The transmittivity value, T, which satisfies both equations causes all the three states ($|1\rangle|1\rangle, |0\rangle|2\rangle$ and $|2\rangle|0\rangle$) to have an equal amplitude, and so their superposition to constitute a Bell-type state.

$$(T-R) = \sqrt{2}\sqrt{TR} \tag{4}$$

$$T + R = 1 \tag{5}$$

Solving the two equations yields:

$$T = 0.211325 \tag{6}$$

$$R = 0.788675 \tag{7}$$

$$\text{Efficiency: } 0.57735 \times \frac{1}{3^2} \tag{8}$$

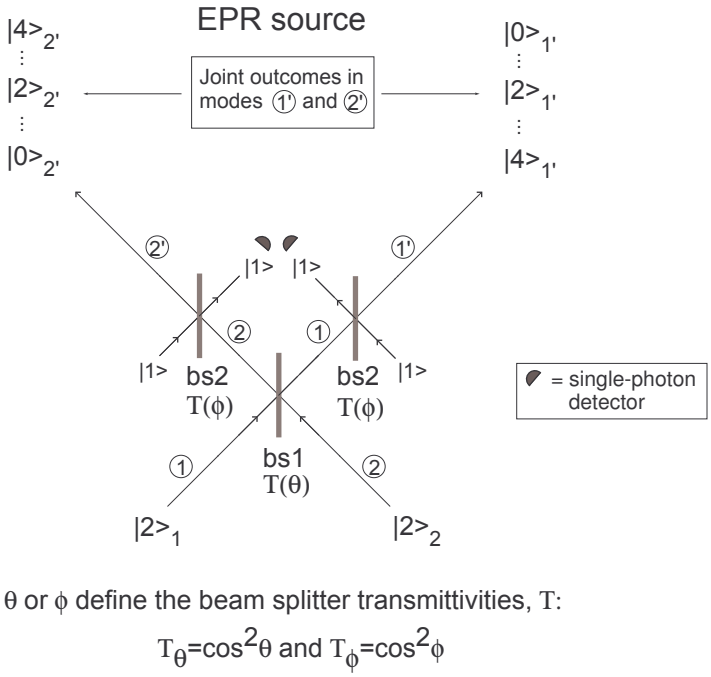

FIG. 4: Encircled numbers $1'$ and $2'$ label specific modes.

Employing a beam splitter of this transmittivity ensures that 60% of the output from our EPR set-up is a maximally entangled state of the form

$$\frac{1}{\sqrt{3}}\big(|20\rangle + |11\rangle + |02\rangle\big).$$

This Bell-type state can then be used in a teleportation scheme for qutrits $(\alpha|0\rangle + \beta|1\rangle + \gamma|2\rangle)$. The normalisation factor $\frac{1}{9}$ comes from the fact that for a qutrit, there are nine possible Bell-states (since $d = 3$ and d^2 is the number of Bell-states), from which we can detect only one.

Input $|2\rangle_1|2\rangle_2$

In the case of the input $|2\rangle_1|2\rangle_2$, we observe an exponential increase in the number of terms in the amplitude prefactors, albeit the number of state vectors increases only polynomially compared to the $|1\rangle_1|1\rangle_2$ input. This is a trend we observe for every consecutive increase in the number of photons. For this reason, we do not show here the complete calculations for the beam-splitter transmittivites, but rather limit ourselves to illustrating the exponential proliferation of terms in the amplitudes. We then give the solutions for the transmittivites required to generate a Bell-state of the form shown in equation 9. The values were computed numerically and can in principle be performed for any n.
An input of $|2\rangle_1|2\rangle_2$ will produce the following Bell-type state:

$$A|4\rangle_{1'}|0\rangle_{2'} + B|3\rangle_{1'}|1\rangle_{2'} + C|2\rangle_{1'}|2\rangle_{2'} + D|1\rangle_{1'}|3\rangle_{2'} + E|0\rangle_{1'}|4\rangle_{2'} \tag{9}$$

where $A = B = C$. By symmetry, D and E are equal to A and B respectively.

Proceeding as in the case for the $|1\rangle_1|1\rangle_2$ input, we express the $|2\rangle_1|2\rangle_2$ in terms of creation operators acting on the vacuum state:

$$|2\rangle_1|2\rangle_2 \equiv \frac{\hat{a}^{\dagger^2}}{\sqrt{2}}\,\frac{\hat{b}^{\dagger^2}}{\sqrt{2}}\,|0\rangle_1|0\rangle_2$$

where $\hat{a}^\dagger$ and $\hat{b}^\dagger$ act on modes 1 and 2 respectively. The action of beam-splitter $bs1$ is expressed using the convention outlined in figure 3 and leads to the expansion

$$\overset{bs1}{\longmapsto} \frac{1}{2}\left(\sqrt{T}\,\hat{a}^\dagger + \sqrt{R}\,\hat{b}^\dagger\right)^2\left(-\sqrt{R}\,\hat{a}^\dagger + \sqrt{T}\,\hat{b}^\dagger\right)^2|0\rangle|0\rangle$$

Following the action of $bs1$, the overall state is incident on a second beam-splitter, $bs2$, where a second transformation is applied:

$$\overset{bs2}{\longmapsto} \frac{1}{2}\left[\left(\sqrt{T}\left(\sqrt{T}\,\hat{a}^\dagger + \sqrt{R}\,\hat{b}^\dagger\right) + \sqrt{R}\left(-\sqrt{R}\,\hat{a}^\dagger + \sqrt{T}\,\hat{b}^\dagger\right)\right)^2\right.$$

$$\left.+\left(-\sqrt{R}\left(\sqrt{T}\,\hat{a}^\dagger + \sqrt{R}\,\hat{b}^\dagger\right) + \sqrt{T}\left(-\sqrt{R}\,\hat{a}^\dagger + \sqrt{T}\,\hat{b}^\dagger\right)\right)^2\right]|0\rangle|0\rangle$$

Expanding the expression leads to exponents of 4 in $\hat{a}^\dagger$ and $\hat{b}^\dagger$ in addition to cross-terms. It can readily be noticed that the number of terms in the expression has increased exponentially on the preceding simple input $|1\rangle_1|1\rangle_2$.

In the set-up shown in figure 4, we have only two different transmittivities, T_θ and T_ϕ. Their values are calculated by solving simultaneously the expressions for the amplitude prefactors A, B, C for the output states

$$A|4\rangle_{1'}|0\rangle_{2'}, B|3\rangle_{1'}|1\rangle_{2'}, C|2\rangle_{1'}|2\rangle_{2'}$$

obtained from equation 9. Although it might at first appear that we have three equations and only two variables, A, B, C are in fact only three expressions, which we set to equal one another. We solve them in pairs so that (10) and (11) now constitute a properly formed set of two simultaneous equations. The condition that $C = A$ follows.

$$A = B \tag{10}$$

and

$$B = C \tag{11}$$

We solved the equations numerically, expressing them in terms of trigonometric functions with the advantage that the condition $T + R = 1$ is satisfied automatically.

$$A = -\sqrt{6}\cos^4\phi\,\cos^2\theta\,\left(-1+\cos^2\theta\right)\left(-4+5\cos\phi^2\right)$$

$$B = \sqrt{6}\cos^2\phi\,\sin\theta\,\cos\theta\big(-3+10\cos^2\phi-8\cos^4\phi$$

$$+6\cos^2\theta-20\cos^2\phi\,\cos^2\theta+16\cos^4\phi\,\cos^2\theta\big)$$

$$C = \cos^2\phi\,\left(1-6\cos^2\theta+6cos^4\theta\right)\left(2\sin^2\phi-\cos^2\phi\right)^2$$

where $\cos^2\theta = T_\theta$, $\sin^2\theta = R_\theta$, $\cos^2\phi = T_\phi$ and $R_\phi = \sin^2\phi = R_\phi$.
Solving these expressions for θ and ϕ (i.e. T_θ, T_ϕ) for a symmetrical input of $|2\rangle_1|2\rangle_2$ gives the following transmittivity values (reflectivity is $R = 1 - T$):

$$T_\theta = 0.7236068 \tag{12}$$

$$T_\phi = 0.2763932 \tag{13}$$

$$\text{Efficiency: } 0.2 \times \frac{1}{5^2} \tag{14}$$

This scheme generates a maximally entangled state of the form:

$$\sim \frac{1}{\sqrt{5}}\Big[|40\rangle_{1',2'} + |31\rangle_{1',2'} + |22\rangle_{1',2'} + |13\rangle_{1',2'} + |04\rangle_{1',2'}\Big]$$

The efficiency of producing Bell-type states falls exponentially as the number input states is increased. We saw how increasing the input from $|1\rangle_1|1\rangle_2$ to $|2\rangle_1|2\rangle_2$ led to an exponential rise in the number of other possible outputs. Then, the probability of obtaining the sub-selection (where all the detectors in figure 4 register a single photon) from an exponentially larger group of possible outcomes also falls exponentially. This is apparent as we consider the probabilities of obtaining Bell states from inputs $|3\rangle_1|3\rangle_2$ and $|4\rangle_1|4\rangle_2$.

Summary of results for beam-splitter transmittivities in EPR and BSA schemes

Teleportee	Input	T_θ	T_{ϕ_1}	T_{ϕ_2}	T_{ϕ_3}	Efficiency
qubit	$\|1\rangle\|0\rangle$	0.5				0.25 (with PBS)
qutrit	$\|1\rangle\|1\rangle$	0.211325				0.06415
qupentit	$\|2\rangle\|2\rangle$	0.7236068	0.2763932			0.008
quheptit	$\|3\rangle\|3\rangle$	0.1510043	0.6098260	0.8495319		5.306×10^{-5}
qunit	$\|4\rangle\|4\rangle$	0.2896110	0.5212421	0.8281260	0.0399748	5.4×10^{-9}

TABLE I: Summary of beam-splitter transmittivities required for even number inputs of photons to generate maximally entangled states for use in teleportation schemes for qubits, qutrits, qupentits, quheptits, and qunits. This can be extended to odd number inputs for the teleportation of qutetrits, quhexits, quoctits and beyond to arbitrary-dimentional states, or $|qudit\rangle$.

A "counting" argument and the general scheme for the EPR source

In the examples above for different symmetric photon inputs, a general trend emerges that permits the formulation of a counting argument for the linear optical EPR source we propose.

Let us briefly return to the specific case of the photon input $|1\rangle|1\rangle$ (section) required to produce a Bell-state in a teleportation of a qutrit $(\alpha|0\rangle + \beta|1\rangle + \gamma|2\rangle)$. In the relevant set-up on figure 3 (ii), a Bell-state is generated by a single beam-splitter whose transmittivity, T, is treated as a variable. Thus we have one variable and one equation, (4), which is solved for T with the constraint $(T + R = 1)$ (5).

The next input we considered, $|2\rangle|2\rangle$, was used to generate a Bell-state containing five terms: $A|40\rangle + B|31\rangle + C|22\rangle \pm B|13\rangle \pm A|04\rangle$. The amplitudes of the first two and the last two terms are automatically equal by the symmetry of the scheme (although there may be a phase difference). This leaves us with three expressions for the first three amplitudes (A, B, C). Then, we form two independent equations are formed, $(A = B$ and $B = C)$ with two variables.

We can see that for each additional pair of photons injected into input 1 and 2 (on figure 2), there will be one additional independent equation.

Hence an arbitrary symmetrical injection of $|n\rangle|n\rangle$ photons will give rise to $n + 1$ amplitudes, from which it will be possible to form n independent equations. The number of independent variables, i.e. transmittivities, in those equations is set by the number of different beam splitters we introduce into the scheme. It follows that we require also n independent transmittivities if we are to solve n equations. This requirement is ensured by introducing $2n - 1$ beam-splitters for an input of $|n\rangle|n\rangle$ photons. That is, each branch will consist of n beam splitters, the first of which is shared by the two branches.

Figure 2 shows the proposed set-up for a generic EPR source for a symmetric input of number state in its two branches, labelled 1 and 2.

A note on the scope of our argument: generally, the EPR scheme produces Bell-type states for symmetric inputs of photons ($|n\rangle_1|n\rangle_2$). Maximally entangled states thus produced will have the form expressed in equation 15:

$$\sim \frac{1}{\sqrt{2n+1}}\Big[|2n,0\rangle_{1',2'} + |(2n-1),1\rangle_{1',2'} + \ldots + |n,n\rangle_{1',2'} + \ldots + |1,(2n-1)\rangle_{1',2'} + |0,2n\rangle_{1',2'}\Big] \tag{15}$$

where n is the number of photons injected into each branch (1 and 2) in figure 2.
Such maximally entangled states can be used in teleportation of any pure state with an *odd number* of terms in the superposition: that is, qutrits ($\alpha|0\rangle + \beta|1\rangle + \gamma|2\rangle$), qupentits ($\alpha|0\rangle + \beta|1\rangle + \gamma|2\rangle + \mu|3\rangle + \lambda|4\rangle$), quheptits ($\alpha|0\rangle + \beta|1\rangle + \gamma|2\rangle + \mu|3\rangle + \lambda|4\rangle + \xi|5\rangle + \zeta|6\rangle$) and so on. Generating Bell-type states required to teleport *even number* arbitrary-dimensional pure states, such as quadrits ($\alpha|0\rangle + \beta|1\rangle + \gamma|2\rangle + \mu|3\rangle$)and quhexits ($\alpha|0\rangle + \beta|1\rangle + \gamma|2\rangle + \mu|3\rangle + \lambda|4\rangle + \xi|5\rangle$), requires an asymmetric input in the input channels 1 and 2. However, our EPR scheme allows equally the generation of Bell-type states with asymmetric inputs, which extends the range of teleportee candidates to *even number* superpositions too.

It has been suggested in [41–43] that linear optical elements would prove unamenable to the task of producing maximally entangled states. Our findings suggest that their full potential remains as yet unused and have much to contribute before resorting to non-linear methods and the challenges associated with those.

The main limitation on the higher orders remains the efficiency, which we see fall exponentially for each step increase of the number of photons and optical elements in the system. There is an additional drop in efficiency due to the fact that only one of the Bell-states in any given basis can be identified, going as $\frac{1}{d^2}$ for a d-dimensional teleportee state.

The Bell State Analyser (BSA)

An advantage of the proposed the EPR source is that it can be adapted for use as a Bell state analyser. This follows from the fact that the scheme consists of a series of unitary operations carried out by linear optical elements. If a Bell-state produced by our scheme is then driven back through the system in time-reversal fashion, that is, it undergoes in *reverse sequence* the same operations that produced it (starting with the last operation), we can regain our input states. Thus by inverting our EPR scheme, as shown in figure 5, where the input is now a Bell-state, the outputs are symmetrical numbers of photons from which we can infer which Bell-state is present.

The BSA time-reversal measurement consists of applying the conjugate unitary transformation for every optical element. This means that what were previously the output states in the EPR scheme are now the inputs for the BSA. Broadly, the scheme for generating the maximally entangled states is reversed in the sense of undoing all the unitary transformations in order to know what were its number-state inputs. This is equivalent to knowing what Bell-state was present at the BSA input.

Combining the EPR source and the BSA in teleportation

Figures 6 and 7 show how the two schemes for producing maximally entangled states and then measuring them come together in a complete teleportation set-up.

In the example on figure 6, the EPR source generates by a series of unitary transformations $\mathbf{U}$, the maximally entangled state required for the teleportation of a qutrit. This is followed by a Bell-state analysis performed by the BSA, which reverses the EPR source's operations by applying the conjugate transformation $\mathbf{U}^\dagger$. Here, $\mathbf{U}$ and $\mathbf{U}^\dagger$ represent all the individual operations performed by each optical element in the scheme that produces and measures the Bell state. This set-up has the property of being symmetrical, which lends it more readily to implementation. Here, the EPR source takes an input of $|1\rangle_1|1\rangle_2$ to generate one of the Bell-type states required for a qutrit, while the BSA in this example "measures" an output $|1\rangle|1\rangle$ with detectors D_l and D_r. This tells us that the Bell state into which the qutrit was projected, must be the one produced by an input of $|1\rangle|1\rangle$ at the EPR source.
A limitation of the scheme is that in its simplest form, the BSA can identify only one of the possible nine Bell states available to a qutrit. This entails a drop in the teleportation efficiency to one-ninth of an ideal BSA. However, using a polarising beam-splitter (PBS) can help to improve efficiency, although this would still not remove the exponential

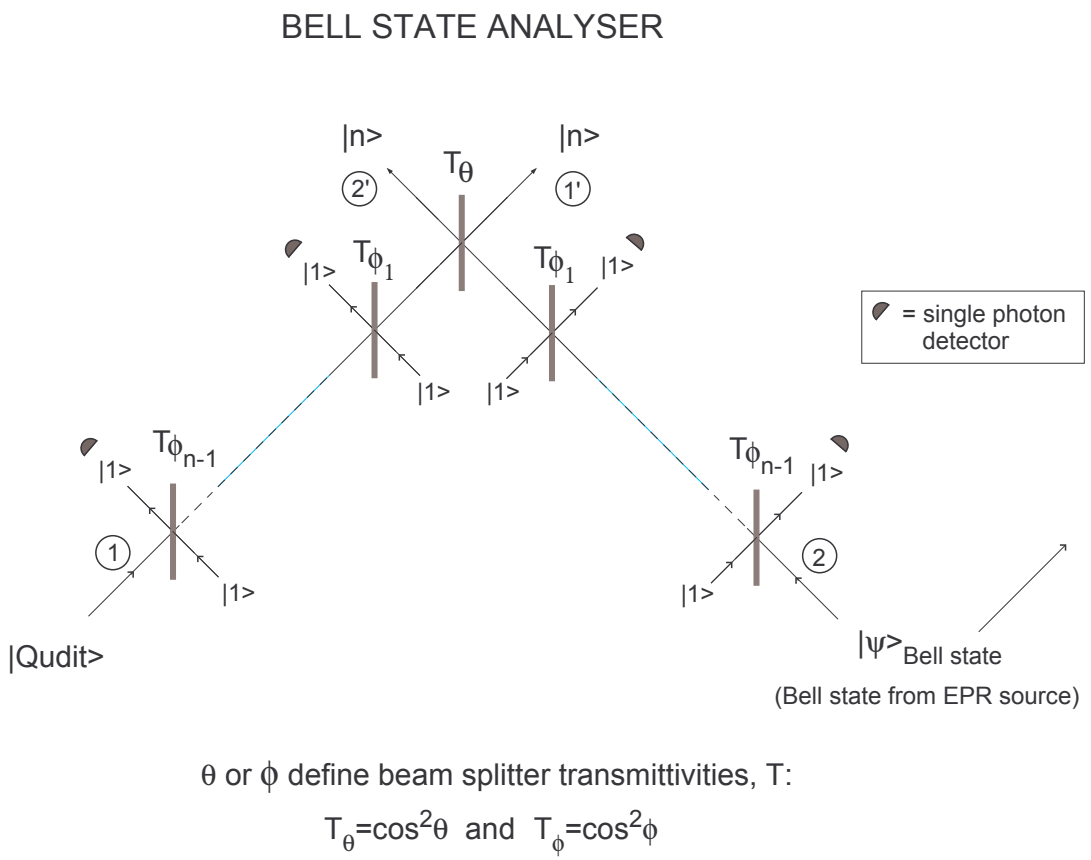

FIG. 5: Schematic of the Bell state analyser (BSA), reversing all unitary operations performed by the EPR source. A Bell state can be identified by the number of photons at the outputs labelled $1'$ and $2'$. For any given Bell state produced by our EPR source, the outputs of the BSA would give back exactly the number of photons used as inputs for the EPR source.

decay in efficiency for higher dimensional states.

Our teleportation scheme can be generalised to an arbitrary-dimensional pure state, or $|qudit\rangle$ (figure 7(b)) since our EPR source can ensure a supply of maximally entangled states of the correct form, while the BSA applies the reverse operation. However, the teleportation efficiency is highly sensitive to the dimension of the qudit, showing an exponential drop the larger the qudit. This is a consequence of the exponential fall in the efficiency of producing and detecting the Bell-states for large qudit dimensions. The efficiency of the BSA falls also exponentially, since the measurement process is merely the reverse of the production sequence. However, this problem can be avoided by keeping to relatively low-dimensional qudits, and in particular, input states up to say $|2\rangle|2\rangle$ are well within experimental reach.

Another practical difficulty in the implementation of the teleportation scheme is the challenge of single-photon detection. One way of detecting single-photons using avalanche photodiodes or photomultipliers, would be to introduce further cascades of symmetric beam-splitters at the outputs. A "click" in a detector does not tell us whether one, two or maybe three photons were incident simultaneously. By introducing a symmetric beam-splitter into a beam consisting of say two photons, we double the probability that the "click" is caused by a single photon. Introducing yet another beam-splitter would further increase the detection reliability, albeit at the expense of the overall efficiency of the scheme. However, this has become much less of a problem in recent years with the advent of highly efficient, low-noise, single-photon detectors.

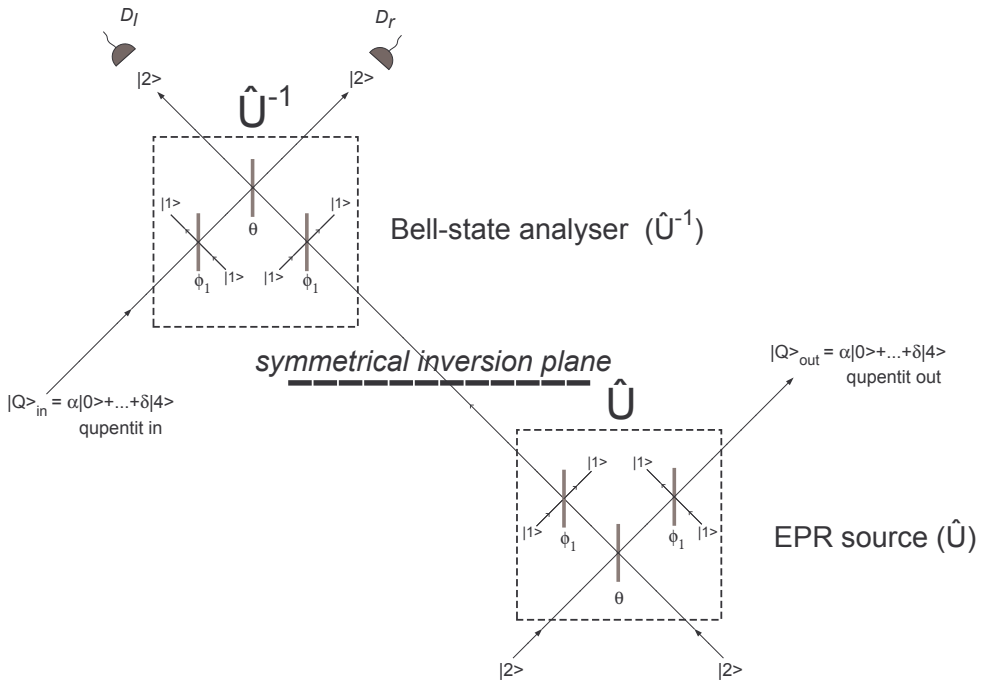

FIG. 6: Schematic showing how the two schemes for producing maximally entangled states and then measuring come together in a complete teleportation set-up. Since the EPR source consists of a sequence of unitary operations **U**, then to perform a Bell-measurement, the BSA need only apply the conjugate transformations in a time-reverse, $\mathbf{U}^\dagger$, fashion. This makes the scheme symmetrical.

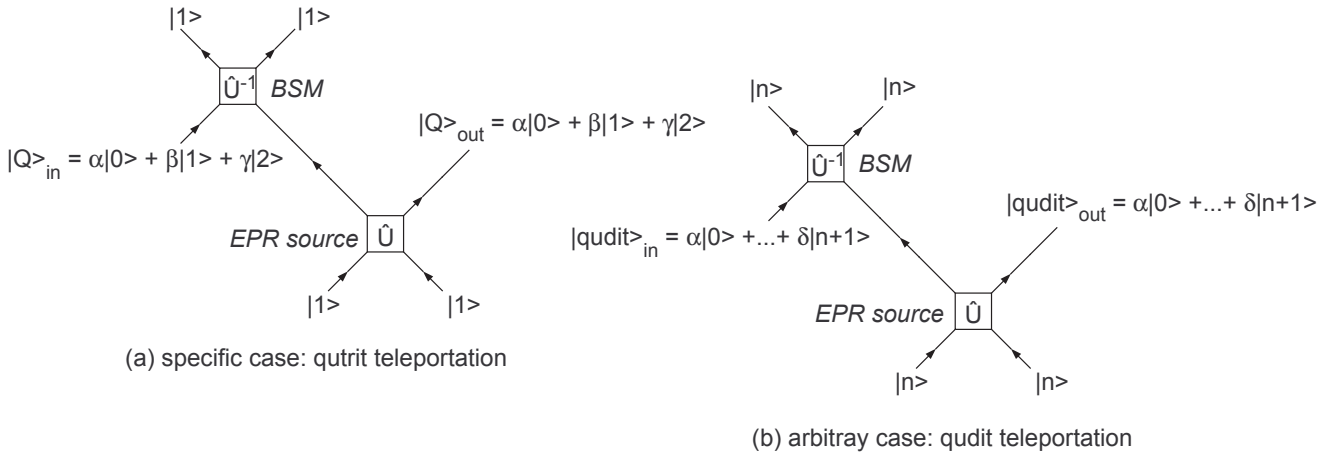

FIG. 7: Teleportation schematic for (a) a qutrit and (b) an arbitrary-dimensional pure state, $|qudit\rangle$. The EPR source ensures that the Bell-state required for the qudit is produced, while the BSA applies the reverse operation to measure the Bell state. As the dimension of the qudit increases, the efficiency of teleportation falls exponentially.

Concluding remarks

We began by introducing potential applications of number-state teleportation as an effective method of information transfer in the context of quantum information processing. We took as our starting point a qubit teleportation protocol that we extended to an arbitrary dimensional number states, using linear optical elements exclusively. To this end, we presented a procedure for generating maximally entangled states on demand and of the required dimension, by using a cascade of beam-splitters arranged cross-beam fashion along two axes in a symmetrical "V"

layout. The key aspect of our EPR scheme relied on treating the sequence of beam-splitter transmittivities along each axis as variables. Their values were determined by the solutions to a set simultaneous equations representing the amplitudes for the sub-selection of number states forming the desired Bell-type state. It was then shown how the scheme for the EPR source could easily be adapted for use as a Bell-state analyser when implemented in a time-reversal manner. Finally, it was demonstrated that when the output of the EPR scheme is used as the input to the BSA, we have a complete teleportation set-up for arbitrary dimensional number-states.

Consideration was also given to the challenges associated with implementing this scheme. Teleportation efficiency decays exponentially for stepwise increases in the number-state dimension. This difficulty can be avoided by using lower-dimensional states. In terms of applications, it is unlikely that high-dimensional state teleportation would find wide use, partly because of the technical difficulty of preparing large pure states (i.e. the states to be teleported). However, towards the lower-dimensional end, say, for qutrits, the teleportation method proposed here maintains a high efficiency (see section for summary of values). It would would be worthwhile to see the scheme implemented experimentally as it would mark a practical milestone on the to quantum communication.

Acknowledgements

The authors thank Časlav Brukner for discussions, and the Oxford Martin School and National Research Foundation Singapore for financial support.

[1] Pirandola, S. et al. Advances in quantum teleportation, Nat. Phot. 641, 9 (2016).
[2] Bouwmeester, D. et al. Experimental quantum teleportation. Nature 390, 575579 (1997).
[3] Boschi, D. et al, Phys. Rev. Lett. 80, 1121-1125 (1998)
[4] Braunstein, S. L. and van Loock, P. Quantum information theory with continuous variables. Rev. Mod. Phys. 77, 513577 (2005).
[5] E. Lombardi, F. Sciarrino, S. Popescu, F. De Martini, Teleportation of a vacuum-one-photon qubit, Phys. Rev. Lett.**88**(7) (2001).
[6] Bennett, C. H. et al., Teleporting an unknown quantum state via dual classical and Einstein-Podolsky-Rosen channels, Phys.Rev.Lett.**70**(13), 1895 (1993).
[7] Barrett, M. D. et al. Deterministic quantum teleportation of atomic qubits. Nature 429, 737739 (2004).
[8] Riebe, M. et al. Deterministic quantum teleportation with atoms. Nature 429, 734737 (2004).
[9] Riebe, M. et al. Quantum teleportation with atoms: Quantum process tomography. New J. Phys. 9, 211 (2007).
[10] Olmschenk, S. et al. Quantum teleportation between distant matter qubits. Science 323, 486489 (2009).
[11] Noelleke, C. et al. Efficient teleportation between remote single-atom quantum memories. Phys. Rev. Lett. 110, 140403 (2013).
[12] Sherson, J. F. et al. Quantum teleportation between light and matter. Nature 443, 557560 (2006).
[13] Krauter, H. et al. Deterministic quantum teleportation between distant atomic objects. Nature Phys. 9, 400404 (2013).
[14] Chen, Y.-A. et al. Memory-built-in quantum teleportation with photonic and atomic qubits. Nature Phys. 4, 103107 (2008).
[15] Bao, X.-H. et al. Quantum teleportation between remote atomic-ensemble quantum memories. Proc. Natl Acad. Sci. USA 109, 2034720351 (2012).
[16] Gao, W. B. et al. Quantum teleportation from a propagating photon to a solid-state spin qubit. Nature Commun. 4, 2744 (2013).
[17] Bussires, F. et al. Quantum teleportation from a telecom-wavelength photon to a solid-state quantum memory. Nature Photon. 8, 775778 (2014).
[18] Steffen, L. et al. Deterministic quantum teleportation with feed-forward in a solid state system. Nature 500, 319322 (2013).
[19] Pfaff, W. et al. Unconditional quantum teleportation between distant solid-state quantum bits. Science 345, 532535 (2014).
[20] Nielsen, M. A., Knill, E. and Laflamme, R. Complete quantum teleportation using nuclear magnetic resonance. Nature 396, 5255 (1998).
[21] Furusawa, A. et al. Unconditional quantum teleportation. Science 282, 706709 (1998).
[22] Bowen, W. P. et al. Experimental investigation of continuous-variable quantum teleportation. Phys. Rev. A 67, 032302 (2003).
[23] Zhang, T. C., Goh, K. W., Chou, C. W., Lodahl, P. and Kimble, H. J. Quantum teleportation of light beams. Phys. Rev. A 67, 033802 (2003).
[24] Takei, N., Yonezawa, H., Aoki, T. and Furusawa, A. High-fidelity teleportation beyond the no-cloning limit and entanglement swapping for continuous variables. Phys. Rev. Lett. 94, 220502 (2005).
[25] Yonezawa, H., Braunstein, S. L. and Furusawa, A. Experimental demonstration of quantum teleportation of broadband squeezing. Phys. Rev. Lett. 99, 110503 (2007).

[26] Takei, N. et al. Experimental demonstration of quantum teleportation of a squeezed state. Phys. Rev. A 72, 042304 (2005).
[27] Lee, N. et al. Teleportation of nonclassical wave packets of light. Science 332, 330333 (2011).
[28] Yukawa, M., Benichi, H. and Furusawa, A. High-fidelity continuous-variable quantum teleportation toward multistep quantum operations. Phys. Rev. A 77, 022314 (2008).
[29] Takeda, S., Mizuta, T., Fuwa, M., van Loock, P. and Furusawa, A. Deterministic quantum teleportation of photonic quantum bits by a hybrid technique. Nature 500, 315318 (2013).
[30] Ursin, R. et al. Quantum teleportation across the Danube. Nature 430, 849 (2004).
[31] Boschi, D., Branca, S., De Martini, F., Hardy, L. and Popescu, S. Experimental realisation of teleporting an unknown pure quantum state via dual classical and EinsteinPodolskiRosen channels. Phys. Rev. Lett. 80, 11211125 (1998).
[32] Jin, X.-M. et al. Experimental free-space quantum teleportation. Nature Photon. 4, 376381 (2010).
[33] Kim, Y.-H., Kulik, S. P. and Shih, Y. Quantum teleportation of a polarisation state with complete Bell state measurement. Phys. Rev. Lett. 86, 13701373 (2001).
[34] Yin, J. et al. Quantum teleportation and entanglement distribution over 100-kilometre free-space channels. Nature 488, 185188 (2012).
[35] Ma, X.-S. et al. Quantum teleportation over 143 kilometres using active feed-forward. Nature 489, 269273 (2012).
[36] Wang, X.-L. et al. Quantum teleportation of multiple degrees of freedom in a single photon. Nature 518, 516519 (2015).
[37] Ma, X.-S. et al. Quantum teleportation over 143 kilometres using active feed-forward, Nature 489, 269273 (2012).
[38] Einstein, A., Podolsky, B., Rosen, N., Phys. Rev. **47**, 777-780, (1935).
[39] Wootters, W. K. and W. H. Zurek, W. H., A single quantum cannot be cloned Nature 299, 802 (1982).
[40] Walther, P. and Zeilinger, A., Experimental realization of a photonic Bell-state analyzer, Phys. Rev. A 72, 010302 (2005).
[41] E. Knill, R. Laflamme, G. Milburn, Nature (London), A scheme for efficient quantum computation with linear optics, 409, 4652 (2001).
[42] Calsamiglia, J., Generalised measurements by linear elements, Phys.Rev.A, **65**, (2002).
[43] Calsamiglia, J., Luetkenhaus, N., Maximum efficiency of a linear-optical Bell-state analyzer, App. Phys. B, **72(1)**, 67-71 (2001).
[44] S. Scheel, N. Luetkenhaus, Upper bounds on success probabilities in linear optics, New J. of Phys., 6 (2004).